Journal of Photonics for Energy

SPIEDigitalLibrary.org/jpe

Self-assembled thienylsilane molecule as interfacial layer for ZnO nanowire/polymer hybrid system

Tingting Xu
Qiliang Chen
Dai-Hong Lin
Hsueh-Yu Wu
Ching-Fuh Lin
Qiquan Qiao

SPIE

Self-assembled thienylsilane molecule as interfacial layer for ZnO nanowire/polymer hybrid system

Tingting Xu,[a] Qiliang Chen,[a] Dai-Hong Lin,[b] Hsueh-Yu Wu,[b] Ching-Fuh Lin,[b] and Qiquan Qiao[a]

[a] South Dakota State University, Center for Advanced Photovoltaics, Department of Electrical Engineering, 0020 SECS, Brookings, South Dakota 57007

[b] National Taiwan University, Institute of Photonics and Optoelectronics, Department of Electrical Engineering, Taipei, 10617, Taiwan

Qiquan.Qiao@sdstate.edu

Abstract. A thienylsilane molecular layer is self-assembled onto vertically aligned ZnO nanowire templates for promoting *in situ* electrochemical polymerization of P3HT. The silane functionalization on ZnO surface is investigated using x-ray photoelectron spectroscopy and water contact angle measurements. The silane-based surface modified layer acts as a favorable nucleation site for electrochemical polymerization. We find that the oxidation potential for electrochemical polymerization is obviously decreased compared to that without a surface modifier. The UV-visible absorption in the ZnO nanowire/P3HT film with thienylsilane molecular layer is much stronger than that without surface modification. [DOI: 10.1117/1.3554662]

Keywords: *in situ* polymerization; electropolymerization; surface modification.

Paper 10148SSR received Aug. 16, 2010; revised manuscript received Jan. 12, 2011; accepted for publication Jan. 25, 2011; published online Mar. 10, 2011.

1 Introduction

Polymer hybrid solar cells consisting of conjugated polymers as electron donor and nanostructured inorganic semiconductors as electron acceptor are promising candidates for generating electricity. They have attracted extensive attention[1–6] because they may combine the advantages of both sides: solution processing of polymers and high electron affinity/transport of inorganic semiconductors. In addition to the widely used polymer/fullerene solar cells,[7] hybrid organic/inorganic solar cells offer another opportunity to develop a new generation of low-cost solar cells for high performance. The interfacial area between donor and acceptor can also be greatly enhanced by using a variety of solution processable polymers and nanostructured materials.[8] Extensive work has already been reported that has demonstrated the promise of combining conjugated polymers with various nanostructured inorganic materials, such as CdSe,[1,9,10] TiO_2,[11–14] ZnO,[15,16] and Si.[17]

In physically blended polymer-inorganic hybrid solar cells, although charge separation has been improved,[8,18] it is still difficult to control the composite morphology in order to provide an efficient charge transport via inorganic nanocrystals. To overcome this drawback, ordered heterojunction was tried by utilizing one-dimensional (1-D) inorganic semiconductors to realize a continuous charge transport pathway. 1-D inorganic nanostructured templates, including nanorods, nanotubes, and nanowires, vertically aligned on a substrate have a unique design with nanoscale dimensions. In order to achieve an efficient polymer filling and charge transfer from conjugated polymers to inorganic semiconductors, *in situ* polymerization starting from monomers has been used rather than physically filtrating long chain polymers directly into the

1947-7988/2011/$25.00 © 2011 SPIE

nanostructures.[19] The monomers have a much smaller size than the nanopores in the inorganic nanostructured template and could significantly improve infiltration. Additionally, chemical modification of the surface of inorganic materials (e.g., TiO_2, ZnO, etc.) could create a more favorable surface energy.[20] Phosphonic acid[21] and amine moieties[22] have been used as an interfacial molecular layer between the donor and acceptor. Zhang et al. reported that a chemical oxidative polymerization has been applied to *in situ* polymerize P3HT inside a surface-initiated TiO_2 nanotube template, and their results showed improved photophysical properties compared to the physically filtrated samples.[19] Tepavcevic et al. used UV irradiation to grow P3HT and found that the photocurrent response was more enhanced than that in the samples made by physical filtration.[20]

In this study, P3HT was *in situ* polymerized onto a ZnO nanowire acceptor template by electrochemical polymerization through a thienylsilane linker. The ZnO nanowires were grown perpendicularly onto an ITO substrate from aqueous solution at low temperature. The electrochemical polymerization of P3HT was conducted on clean ITO substrate, ZnO nanowire surface with and without a silane linker, respectively. The silane linker was capped with a thiophene ring to improve the interaction between P3HT and ZnO nanowires. The results show that the thienylsilane modified layer obviously decreased the oxidation potential for the electrochemical polymerization of P3HT.

2 Experiment Methods

Anhydrous toluene and acetonitrile were purchased from Acros (Morris Plains, NJ, USA). Triethoxy-2-thienylsilane and tetrabutylammonium hexafluorophonate (Bu_4NFP_6, electrochemical grade) were obtained from Sigma Aldrich (St. Louis, MO, USA). They were used as received. Chloroform was dried by CaH_2. All the other solvents were ordered from commercial sources and used without further purification. 3-hexylthiophene was synthesized according to a literature method.[23]

ZnO nanowires were prepared by a method reported previously.[24] They were vertically aligned on an ITO substrate with a hexagonal shape of an average diameter of ~50 nm. ZnO nanoparticle (NP) films were prepared by spin-coating the solution of 0.75 M zinc acetate dehydrate, 0.75 M ethanol amine, and 2-methoxyethanol solution for multiple times, followed by annealing the films at 350°C for 2 h.

Scanning electron microscopy (SEM) was performed via Hitachi S-4300N SEM at an accelerating voltage of 10 kV at room temperature. Water contact angle images were taken from a Video Contact Angle 2000 system via sessile drop method. O_2 plasma cleaning was done using PDC-32G plasma cleaner (Harrick Plasma). Cyclic voltammetry (CV) experiments were conducted with an Ametek versa SATA 3 instrument. X-ray photoelectron spectroscopy (XPS) measurements were performed on an SSX-100 system (Surface Science Instruments) equipped with a monochromated Al Kα x-ray source, a hemispherical sector analyzer, and a resistive anode detector. UV-visible (UV-Vis) absorption spectra were obtained on an HP Agilent 8352 UV-Vis spectrophotometer.

2.1 *Surface-Modification of ZnO Nanowires*

The surface modification of ZnO nanowires was conducted following a reported method.[25] The ZnO nanowire template was placed into an O_2 plasma cleaner for 15 min to promote hydroxylation with the ZnO side facing up. A silane solution was freshly prepared by mixing triethoxy-2-thienylsilane molecules with toluene and *n*-butylamine catalyst. The solution was preheated at 45°C for 30 min, and then the pretreated ITO/ZnO nanowire substrate was immersed into the heated solution. After that, the ITO/ZnO nanowire substrate was removed from the solution and rinsed with toluene and acetone, and dried with N_2. Postcuring was done at 110°C.

2.2 *Electrochemical Polymerization*

An enclosing homemade glass cell was installed using a standard three-electrode configuration with an Ag/AgCl as the reference electrode and a coiled platinum auxiliary electrode as the counter electrode. Different substrates, including ITO and ITO/ZnO nanowires with and without surface modification, served as the working electrode, respectively. CV experiments were conducted at room temperature. The electrolyte consisting of Bu_4NFP_6 (0.1 M) and 3-hexylthiophene (3HT) monomer (0.005 M) in an anhydrous acetonitrile solution was freshly prepared. The maximum applied potentials for electrochemical polymerization were varied from 1.5 to 2.2 V with a scan rate of 0.1 V/s for each. The final films grown on the ZnO surface were washed with ethanol, acetone and then dried by N_2.

3 Results and Discussion

3.1 *Surface Modification of ZnO Nanowires*

Figure 1 shows the SEM images of the ZnO nanowires. It can be seen that the prepared ZnO nanowires have an average diameter of $\sim$50 nm and a length of $\sim$1 μm. They are uniformly distributed on the ITO substrate.

The electrochemical polymerization method is an easy and cheap method to obtain polymers. In addition, it does not require polymers to have a side chain for solubility. In order to grow polymers by the electrochemical method, the conductive substrates are required; however this can be a further advantage for solar cell application because solar cells are fabricated using conducting substrate as electrode, such as ITO, FTO-coated glass, or plastic substrates. There has been extensive work in the electrochemical polymerization field; polythiophene,[26–28] polypyrrole,[29] and poly(3,4-ethylenedioxythiophene)[30] have been electrochemically polymerized and well studied. One disadvantage for electrochemical polymerization method on conducting substrate is that it initiates the polymerization reaction at the electrode surface rather than that of the semiconducting oxide (e.g., ZnO),[20] and therefore, it may lead to a large amount of polymer formed on the substrate (electrode) rather than directly onto the semiconducting oxide. To solve this issue, the ZnO nanowires were surface modified by a layer of thienylsilane molecules capped with a thiophene ring that may promote *in situ* polymerization of P3HT on the ZnO nanowire surface. It would possibly help to form a homogeneous layer of P3HT directly attached onto the ZnO nanowire surface. Figure 2 (a $\rightarrow$ b) shows the process of surface functionalization of ZnO nanowires using a thienylsilane molecule, followed by the formation of P3HT synthesized by *in situ* electrochemical polymerization (b $\rightarrow$ c).

After the surface functionalization, the ZnO nanowire templates were characterized by XPS measurement as shown in Fig. 3. The chemical nature and surface energy of ZnO nanowires are expected to change after the modification. Figure 3(a) is the wide-range survey spectrum. The

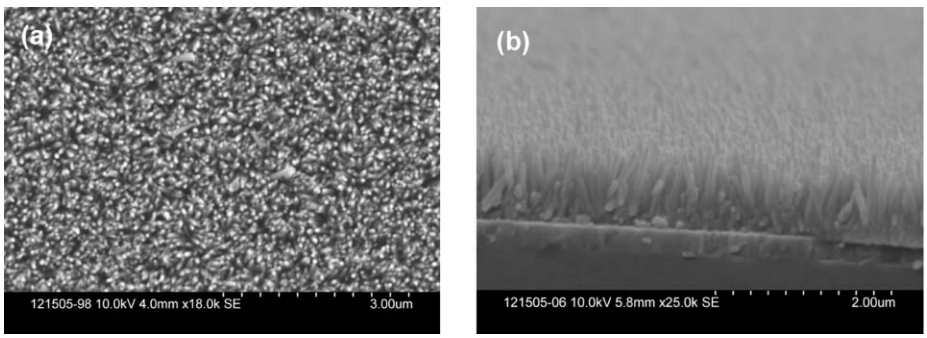

Fig. 1 (a) Top view and (b) tilted cross-sectional SEM image of the ZnO nanowires grown on an ITO substrate.

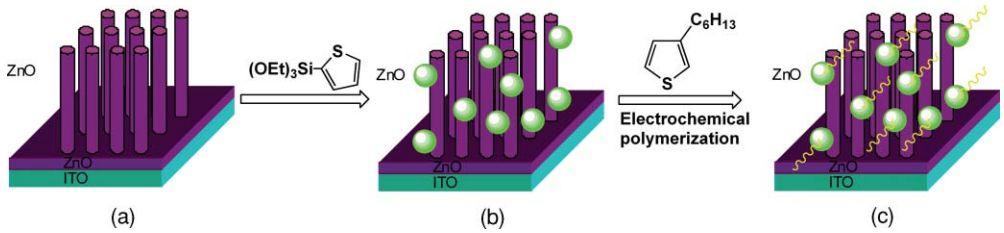

Fig. 2 Procedure to functionalize the ZnO nanowires using triethoxy-2-thienylsilane and then electrochemically polymerize P3HT directly onto the ZnO nanowire surface.

C (1s) signals containing three components at 285.000, 286.666, and 288.921 eV were fitted by Gaussian–Lorentzian functions. From the XPS spectra, the Si (2p) emission around 103.0 eV was found to be weak, but it could still be identified in Fig. 3(b). This confirms that the silane molecular layer formed on ZnO surface.

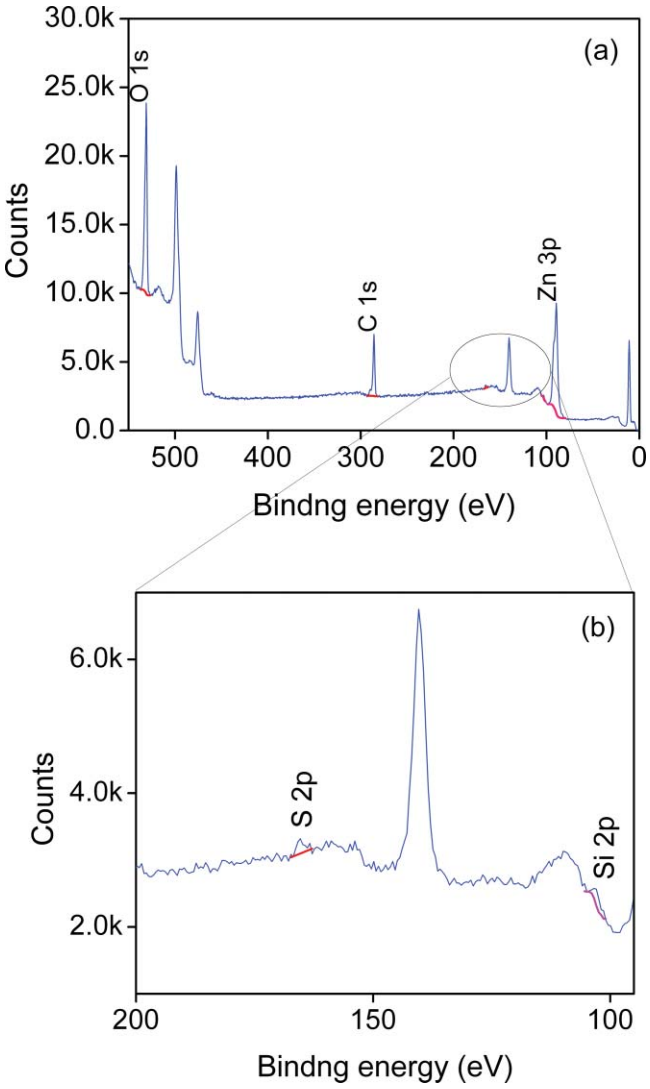

Fig. 3 (a) XPS survey spectrum of thienylsilane modified ZnO nanowires and (b) zoomed XPS in the binding energy of 100–200 eV region that shows the Si (2p) signal.

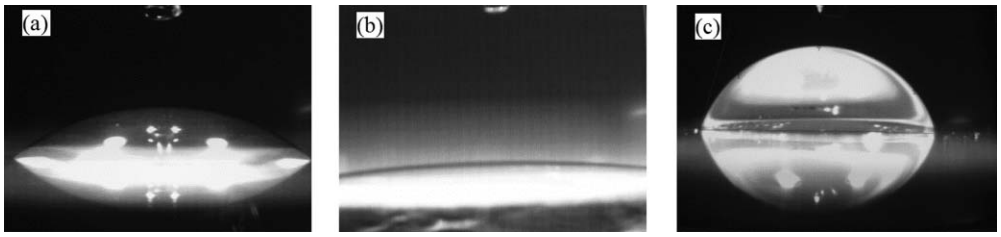

Fig. 4 WCA measurements of (a) ZnO NP film, (b) ZnO NP film treated with O_2 plasma, and (c) surface-modified ZnO NP film via silanization.

To further identify the surface modification on ZnO nanowires, water contact angle (WCA) measurements were conducted to monitor the surface properties of ZnO samples before and after surface modification. Because the surface properties of nanowires are difficult to be studied directly by this method, the ZnO NP films were prepared and measured instead. This method can be a good indicator to monitor the properties of surface-modified ZnO films. At least two samples were tested, and no less than five spots on each sample were examined to ensure accurate measurements. Figure 4 shows the WCA results of the surface-modification processes. The WCA of the pristine ZnO NP film was around 42 ± 2 deg [Fig. 4(a)] and it became <20 deg [Fig. 4(b)] after the O_2 plasma treatment, which caused a hydrophilic ZnO surface. This result is consistent with the O_2 plasma-treated ZnO film reported by others.[25,31,32] Such hydroxylated treatment can promote the reactivity of ZnO sample with the silane reagent. After the silanization reaction, a WCA of 75 ± 2 deg [Fig. 4(c)] was observed from multiple spots on different slides. This data are quite similar to the phenyltriethoxysilane $C_6H_5Si(OCH_2CH_3)_3$ (PTES)-modified ZnO nanoparticle surface, which has a WCA of 72.5 ± 4.3 deg.[25] This confirmed that the silane molecules attached onto the surface of ZnO films successfully and changed the ZnO surface properties. Because of the hydrophobic nature of the thiophene ring, the contact angle of ZnO sample after silanization increased greatly. In addition, the contact angle of silanized samples kept consistent after several days, which showed this surface modification is quite stable.

3.2 *Electropolymerization of P3HT film on ITO/ZnO nanowire substrate*

In order to study the effect of thienylsilane functionalization treatment on the electrochemical deposition of P3HT, the maximum applied potentials (V_{max}) in the potentiodynamic CV experiments were varied quantitatively on different substrates: (*i*) ITO substrate, (*ii*) ITO/ZnO nanowires without thienylsilane group surface modification, and (*iii*) ITO/ZnO nanowires with thienylsilane group surface modification. In the rest of the work, they will be labeled as ITO, ITO/ZnO, ITO/ZnO/Si, respectively.

P3HT was deposited by sweeping the working electrode potential from 0 to V_{max} (verse Ag/Ag^+) at a scan rate of 0.1 V/s for a specific number of cycles. The representative CV sweeps of growing P3HT on three different substrates (ITO, ITO/ZnO, ITO/ZnO/Si) at a V_{max} of 1.8 and 1.9 V, respectively, are shown in Fig. 5. The evidence for successful P3HT growth was the increase of the anodic and cathodic peak current in each successive cycle. During the experiments, a dark color film was observed to form on the electrodes. By increasing V_{max}, the area beneath each curve was increased, which indicated that more P3HT was formed on the electrode.

As shown in Fig. 5, when the number of cycles increased, the oxidization and reduction were also subsequently changed. When comparing the polymerization under the same V_{max}, the area inside the CV curves was in the order of ITO/ZnO $<$ ITO $<$ ITO/ZnO/Si for both $V_{max} = 1.8$ V and $V_{max} = 1.9$ V. The reason for ITO/ZnO $<$ ITO was that ITO had a conducting surface, but ZnO had a semiconducting surface; therefore, P3HT was easier to be oxidized on the ITO substrate than that of ITO/ZnO substrate. However, compared to the ZnO nanowire

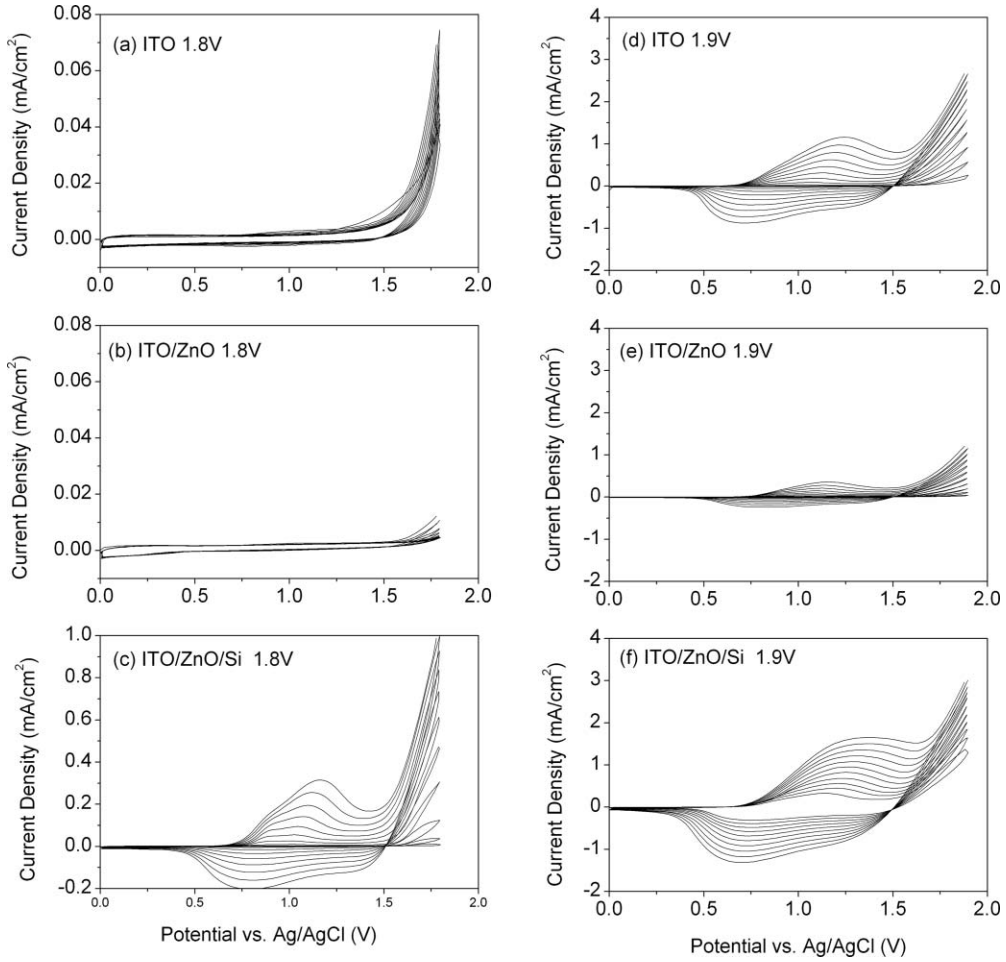

Fig. 5 Cyclic voltammogram of the 3-hexylthiophene monomer at different substrate ITO (a) 1.8 V, (d) 1.9 V; ITO/ZnO (b) 1.8 V, (e) 1.9 V, and ITO/ZnO/Si (c) 1.8 V, (f) 1.9 V.

substrate with thienylsilane surface modification, the P3HT polymerization onset potential was greatly decreased. This indicated that the thienylsilane functionalized ZnO surface acted as a favorable nucleation site for electrochemical polymerization and led to a low-surface electrical potential for nucleation.

For a more quantitative analysis and comparison of the effects of substrates and variations in V_{max} on P3HT growth, the charge density for each curve was calculated. The charge density versus numbers of CV sweeps obtained from the anodic waves were plotted in Fig. 6. It was clearly found that the charge density for ITO and ITO/ZnO substrate changed insignificantly at the V_{max} of 1.8 V. However, it was obviously increased for the ITO/ZnO/Si substrate after the self-assembling of a molecular layer of thienylsilane linker. This further proved that the surface modification could enhance P3HT polymerization at lower potentials.

3.3 *Optical Absorption of Electropolymerized P3HT Film*

Figure 7 shows the UV-visible absorption spectra of the ZnO nanowires and electropolymerized P3HT films with and without thienylsilane surface modification. The ZnO nanowires show absorption up to 375 nm with a characteristic shape. In the presence of P3HT, the absorption was broadened to 650 nm for both the samples of ZnO nanowires with and without surface

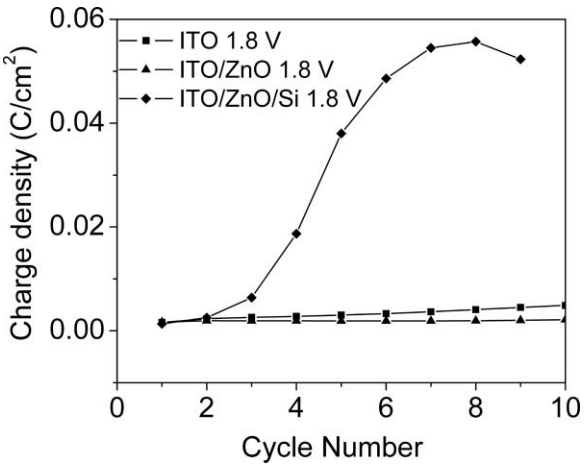

Fig. 6 Charge density versus cycle number calculated from the anodic waves of potentiodynamic CV experiments.

modification. In addition, it was evident that the UV-Vis absorption was much stronger in the sample with the thienylsilane surface modification than the sample without it. The reason is that the thienylsilane-functionalized layer acted as a favorable nucleation site for electrochemical polymerization and caused more P3HT to grow onto ZnO nanowires. This is consistent with the higher charge density found in the sample with thienylsilane surface modification.

4 Conclusions

P3HT was electropolymerized onto the vertically aligned thienylsilane-modified ZnO nanowires. The polymerization onset potential decreased for the ZnO nanowires with thienylsilane group surface modification compared to that of the pristine ZnO nanowires. By increasing the maximum applied potential (V_{max}) for polymerization, an increase in the area beneath each curve indicated that more P3HT was formed. The silane-based surface functionalization acted as a favorable nucleation site for electrochemical polymerization. The UV-Vis absorption in the

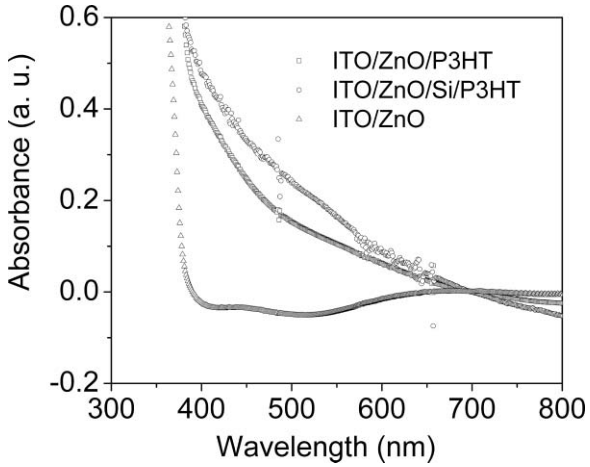

Fig. 7 UV-Vis absorption spectra of ZnO nanowires on an ITO substrate (ITO/ZnO) and electropolymerized P3HT on ZnO nanowires without (ITO/ZnO/P3HT) and with (ITO/ZnO/Si/P3HT) surface modification.

ZnO nanowires with thienylsilane surface modification was much stronger than that for ZnO nanowires without surface modification.

Acknowledgments

This project was partially supported by the National Science Foundation (Grant No. ECCS-0950731), NASA EPSCoR (Grant No. NNX09AP67A), ACS Petroleum Research Funds DNI (Grant No. 48733DNI10), US-Israel Binational Science Foundation (Grant No. 2008265), and U.S.-Egypt Joint Science & Technology Funds (Grant No. 913), the MRSEC Program of the National Science Foundation under Award No. DMR-0819885. The authors also thank Dr. Bing Luo, College of Science and Engineering Characterization Facility, University of Minnesota, for conducting XPS measurement, part of the NSF-funded Materials Research Facilities Network (www.mrfn.org).

References

1. W. U. Huynh, J. J. Dittmer, and A. P. Alivisatos, "Hybrid nanorod-polymer solar cells," *Science* **295**, 2425–2427 (2002).
2. T. Xu, and Q. Qiao, "Conjugated polymer-inorganic semiconductor hybrid solar cells," *Energy Environ. Sci.* (2011), in press.
3. H. Borchert, "Elementary processes and limiting factors in hybrid polymer/nanoparticle solar cells," *Energy Environ. Sci.* **3**, 1682–1694 (2010).
4. I. Gonzalez-Valls, and M. Lira-Cantu, "Vertically-aligned nanostructures of ZnO for excitonic solar cells: A review," *Energy Environ. Sci.* **2**, 19–34 (2009).
5. M. Memesa, S. Weber, S. Lenz, J. Perlich, R. Berger, P. Muller-Buschbaum, and J. S. Gutmann, "Integrated blocking layers for hybrid organic solar cells," *Energy Environ. Sci.* **2**, 783–790 (2009).
6. Y. F. Zhou, M. Eck, and M. Kruger, "Bulk-heterojunction hybrid solar cells based on colloidal nanocrystals and conjugated polymers," *Energy Environ. Sci.* **3**, 1851–1864 (2010).
7. M. Siddiki, J. Li, D. Galipeau, and Q. Qiao, "A review on polymer multijunction solar cells," *Energy Environ. Sci.* **3**, 867–883 (2010).
8. J. Bouclé, P. Ravirajan, and J. Nelson, "Hybrid polymer–metal oxide thin films for photovoltaic applications," *J. Mater. Chem.* **17**, 3141–3153 (2007).
9. S. Dayal, N. Kopidakis, D. C. Olson, D. S. Ginley, and G. Rumbles, "Photovoltaic devices with a low band gap polymer and CdSe nanostructures exceeding 3% efficiency," *Nano Lett.* **10**, 239–242 (2010).
10. W. U. Huynh, X. Peng, and A. P. Alivisatos, "CdSe nanocrystal rods/poly(3-hexylthiophene) composite photovoltaic devices," *Adv. Mater.* **11**, 923–927 (1999).
11. Q. Qiao, and J. T. McLeskey, "Water-soluble polythiophene/nanocrystalline TiO_2 solar cells," *Appl. Phys. Lett.* **86**, 153501 (2005).
12. Q. Qiao, Y. Xie, and J. J. T. McLeskey, "Organic/inorganic polymer solar cells using a buffer layer from all-water-solution processing," *J. Phys. Chem. C* **112**, 9912–9916 (2008).
13. Y.-Y. Lin, T.-H. Chu, S.-S. Li, C.-H. Chuang, C.-H. Chang, W.-F. Su, C.-P. Chang, M.-W. Chu, and C.-W. Chen, "Interfacial nanostructuring on the performance of polymer/TiO_2 nanorod bulk heterojunction solar cells," *J. Am. Chem. Soc.* **131**, 3644–3649 (2009).
14. Q. Qiao, L. Su, J. Beck, and J. T. McLeskey, "Characteristics of water soluble polythiophene:TiO_2 composite and its application in photovoltaics," *J. Appl. Phys.* **98**, 094906 (2005).
15. W. J. E. Beek, M. M. Wienk, and R. A. J. Janssen, "Efficient hybrid solar cells from zinc oxide nanoparticles and a conjugated polymer," *Adv. Mater.* **16**, 1009–1013 (2004).

16. D. J. D. Moet, L. J. A. Koster, B. de Boer, and P. W. M. Blom, "Hybrid polymer solar cells from highly reactive diethylzinc: MDMO–PPV versus P3HT," *Chem. Mater.* **19**, 5856–5861 (2007).
17. S.-C. Shiu, J.-J. Chao, S.-C. Hung, C.-L. Yeh, and C.-F. Lin, "Morphology dependence of silicon nanowire/poly(3,4-ethylenedioxythiophene):poly(styrenesulfonate) heterojunction solar cells," *Chem. Mater.* **22**, 3108–3113 (2010).
18. J. Bouclé, S. Chyla, M. S. P. Shaffer, J. R. Durrant, D. D. C. Bradley, and J. Nelson, "Hybrid solar cells from a blend of poly(3-hexylthiophene) and ligand-capped TiO_2 nanorods," *Adv. Funct. Mater.* **18**, 622–633 (2008).
19. Y. Zhang, C. Wang, L. Rothberg, and M.-K. Ng, "Surface-initiated growth of conjugated polymers for functionalization of electronically active nanoporous networks: Synthesis, structure and optical properties," *J. Mater. Chem.* **16**, 3721–3725 (2006).
20. S. Tepavcevic, S. B. Darling, N. M. Dimitrijevic, T. Rajh, and S. J. Sibener, "Improved hybrid solar cells via *in situ* UV polymerization," *Small* **5**, 1776–1783 (2009).
21. C.-W. Hsu, L. Wang, and W.-F. Su, "Effect of chemical structure of interface modifier of TiO_2 on photovoltaic properties of poly(3-hexylthiophene)/TiO_2 layered solar cells," *J. Colloid Interface Sci.* **329**, 182–187 (2009).
22. W. J. E. Beek, M. M. Wienk, M. Kemerink, X. Yang, and R. A. J. Janssen, "Hybrid zinc oxide conjugated polymer bulk heterojunction solar cells," *J. Phys. Chem. B* **109**, 9505–9516 (2005).
23. D. Appelhans, D. Ferse, H. J. P. Adler, W. Plieth, A. Fikus, K. Grundke, F. J. Schmitt, T. Bayer, and B. Adolphi, "Self-assembled monolayers prepared from ω-thiophene-functionalized *n*-alkyltrichlorosilane on silicon substrates," *Colloids Surf., A* **161**, 203–212 (2000).
24. J.-S. Huang, and C.-F. Lin, "Influences of ZnO sol-gel thin film characteristics on ZnO nanowire arrays prepared at low temperature using all solution-based processing," *J. Appl. Phys.* **103**, 014304 (2008).
25. C. G. Allen, D. J. Baker, J. M. Albin, H. E. Oertli, D. T. Gillaspie, D. C. Olson, T. E. Furtak, and R. T. Collins, "Surface modification of ZnO using triethoxysilane-based molecules," *Langmuir* **24**, 13393–13398 (2008).
26. J. T. Sullivan, K. E. Harrison, J. P. Mizzell, and S. M. Kilbey, "Contact angle and electrochemical characterization of multicomponent thiophene-capped monolayers," *Langmuir* **16**, 9797–9803 (2000).
27. J. P. Correia, and L. M. Abrantes, "*In situ* ellipsometric studies on the electrochemically induced structural modifications during poly(3-methylthiophene) formation," *Synth. Met.* **156**, 287–292 (2006).
28. M. Vignali, R. A. H. Edwards, M. Serantoni, and V. J. Cunnane, "Electropolymerized polythiophene layer extracted from the interface between two immiscible electrolyte solutions: Current-time analysis," *J. Electroanal. Chem.* **591**, 59–68 (2006).
29. C. M. Li, C. Q. Sun, W. Chen, and L. Pan, "Electrochemical thin film deposition of polypyrrole on different substrates," *Surf. Coat. Technol.* **198**, 474–477 (2005).
30. A. I. Melato, A. S. Viana, and L. M. Abrantes, "Different steps in the electrosynthesis of poly(3,4-ethylenedioxythiophene) on platinum," *Electrochim. Acta* **54**, 590–597 (2008).
31. M. D. K. Ingall, C. H. Honeyman, J. V. Mercure, P. A. Bianconi, and R. R. Kunz, "Surface functionalization and imaging using monolayers and surface-grafted polymer layers," *J. Am. Chem. Soc.* **121**, 3607–3613 (1999).
32. B. Zhang, T. Kong, W. Xu, R. Su, Y. Gao, and G. Cheng, "Surface functionalization of zinc oxide by carboxyalkylphosphonic acid self-assembled monolayers," *Langmuir* **26**, 4514–4522 (2010).

Biographies and photographs of the authors not avilable.